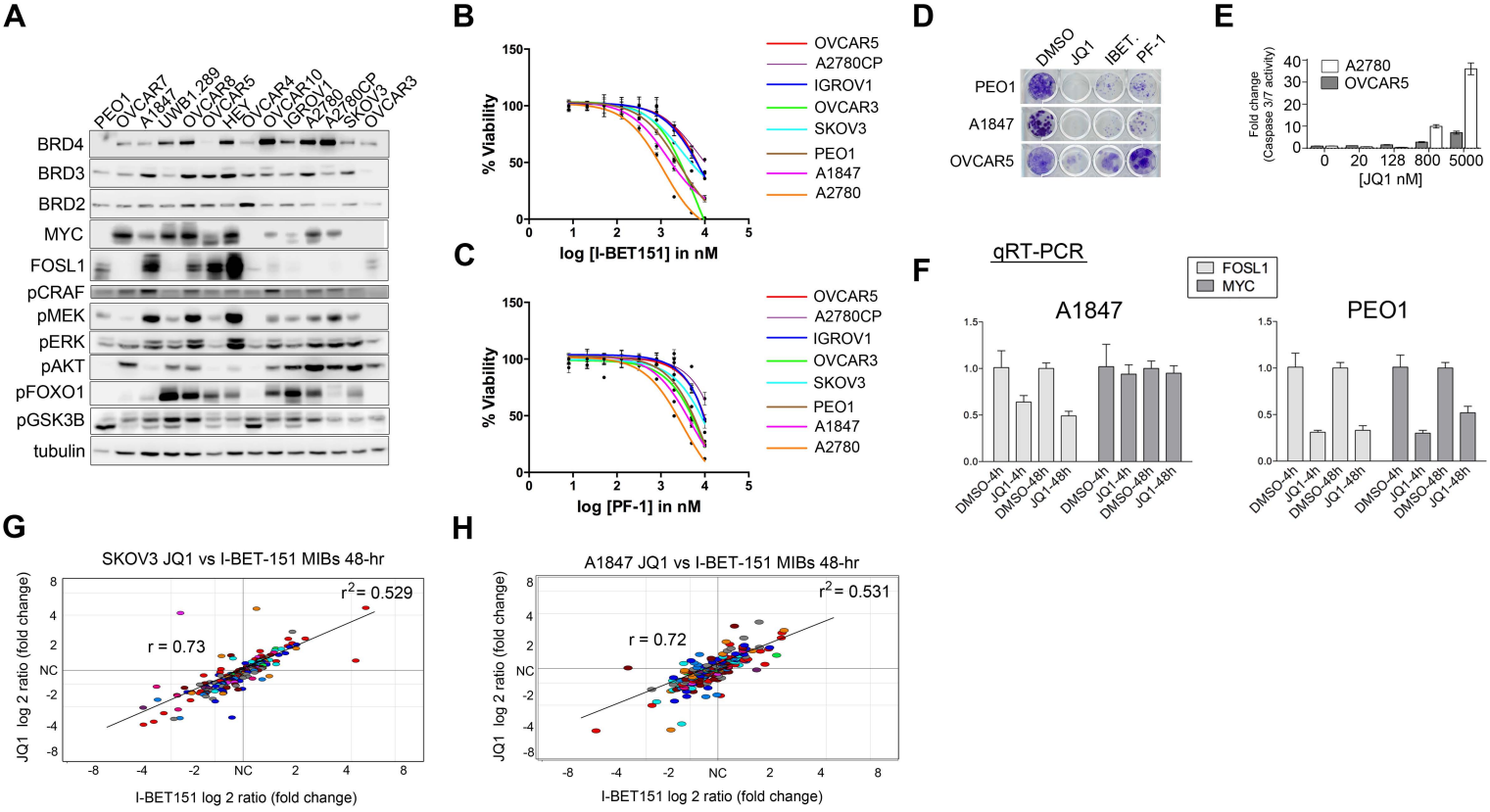
A
PEO1
OVCAR7
A1847
UWB1.289
OVCAR8
OVCAR5
HEY
OVCAR4
OVCAR10
IGROV1
A2780
A2780CP
SKOV3
OVCAR3
BRD4
BRD3
BRD2
MYC
FOSL1
pCRAF
pMEK
pERK
pAKT
pFOXO1
pGSK3B
tubulin
B
% Viability
log [I-BET151] in nM
OVCAR5
A2780CP
IGROV1
OVCAR3
SKOV3
PEO1
A1847
A2780
C
% Viability
log [PF-1] in nM
OVCAR5
A2780CP
IGROV1
OVCAR3
SKOV3
PEO1
A1847
A2780
D
DMSO
JQ1
IBET.
PF-1
PEO1
A1847
OVCAR5
E
Fold change
(Caspase 3/7 activity)
A2780
OVCAR5
[JQ1 nM]
F
qRT-PCR
FOSL1
MYC
A1847
PEO1
DMSO-4h
JQ1-4h
DMSO-48h
JQ1-48h
G
SKOV3 JQ1 vs I-BET-151 MIBs 48-hr
r2= 0.529
r = 0.73
JQ1 log 2 ratio (fold change)
I-BET151 log 2 ratio (fold change)
H
A1847 JQ1 vs I-BET-151 MIBs 48-hr
r2= 0.531
r = 0.72
JQ1 log 2 ratio (fold change)
I-BET151 log 2 ratio (fold change)

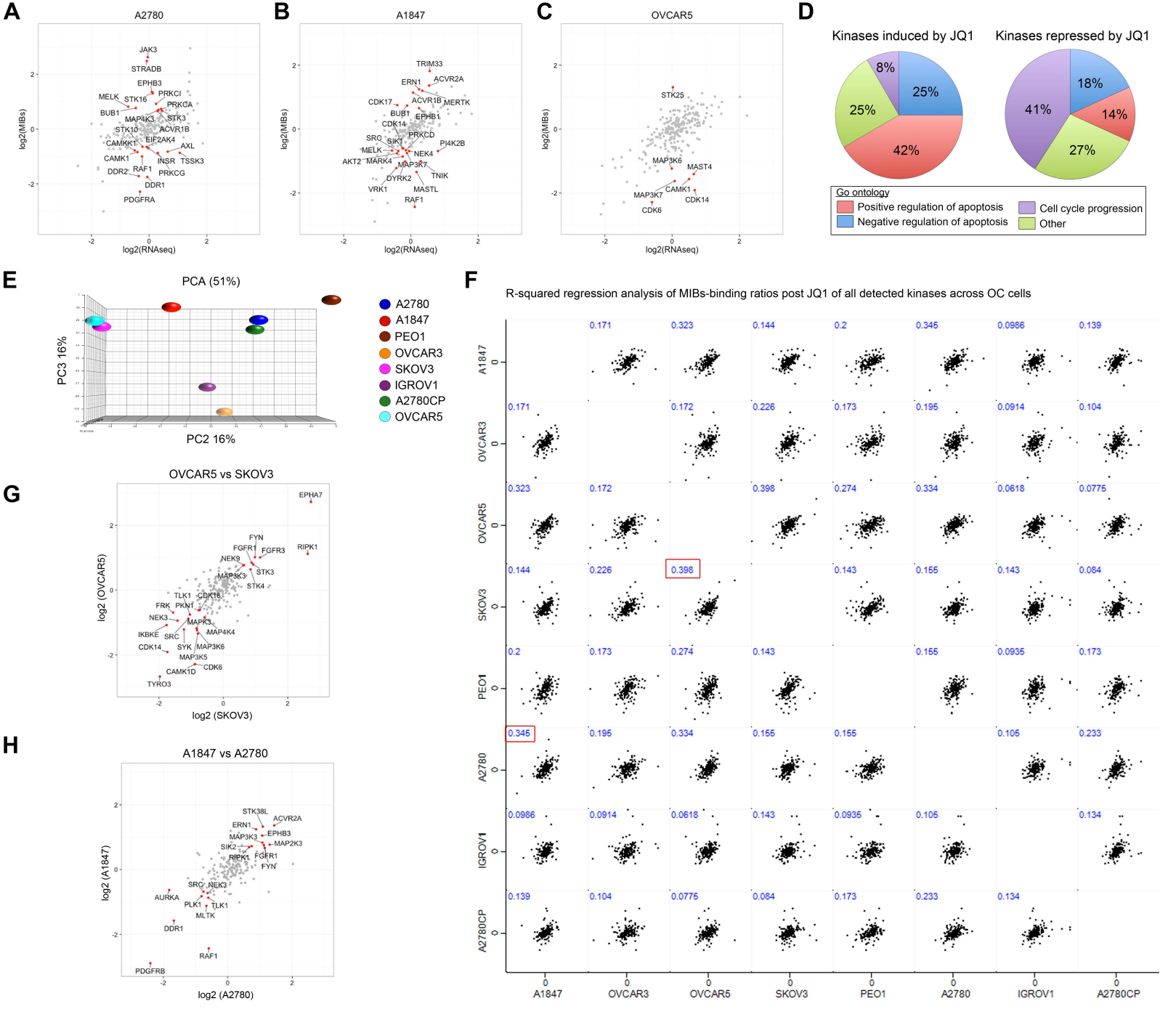
A
A2780
log2(MIBs)
log2(RNAseq)
JAK3
STRADB
EPHB3
PRKCI
MELK
STK16
PRKCA
BUB1
MAP4K3
STK3
STK10
ACVR1B
CAMKK1
EIF2AK4
AXL
CAMK1
INSR
TSSK3
DDR2
RAF1
PRKCG
DDR1
PDGFRA
B
A1847
TRIM33
ERN1
ACVR2A
CDK17
ACVR1B
MERTK
BUB1
EPHB1
CDK14
PRKCD
SRC
SIK1
PI4K2B
MELK
NEK4
AKT2
MARK4
MAP3K7
DYRK2
TNIK
VRK1
MASTL
RAF1
C
OVCAR5
STK25
MAP3K6
MAST4
CAMK1
MAP3K7
CDK14
CDK6
D
Kinases induced by JQ1
8%
25%
25%
42%
Kinases repressed by JQ1
18%
41%
14%
27%
Go ontology
Positive regulation of apoptosis
Negative regulation of apoptosis
Cell cycle progression
Other
E
PCA (51%)
PC3 16%
PC2 16%
A2780
A1847
PEO1
OVCAR3
SKOV3
IGROV1
A2780CP
OVCAR5
F
R-squared regression analysis of MIBs-binding ratios post JQ1 of all detected kinases across OC cells
A1847
OVCAR3
OVCAR5
SKOV3
PEO1
A2780
IGROV1
A2780CP
G
OVCAR5 vs SKOV3
log2 (OVCAR5)
log2 (SKOV3)
EPHA7
FYN
FGFR1
FGFR3
RIPK1
NEK9
STK3
MAP3K3
STK4
TLK1
CDK16
FRK
PKN1
NEK3
MAPK3
IKBKE
SRC
MAP4K4
CDK14
SYK
MAP3K6
MAP3K5
CDK6
CAMK1D
TYRO3
H
A1847 vs A2780
log2 (A1847)
log2 (A2780)
STK38L
ACVR2A
ERN1
EPHB3
MAP3K3
MAP2K3
SIK2
RIPK1
FGFR1
FYN
SRC
NEK3
AURKA
PLK1
TLK1
MLTK
DDR1
RAF1
PDGFRB

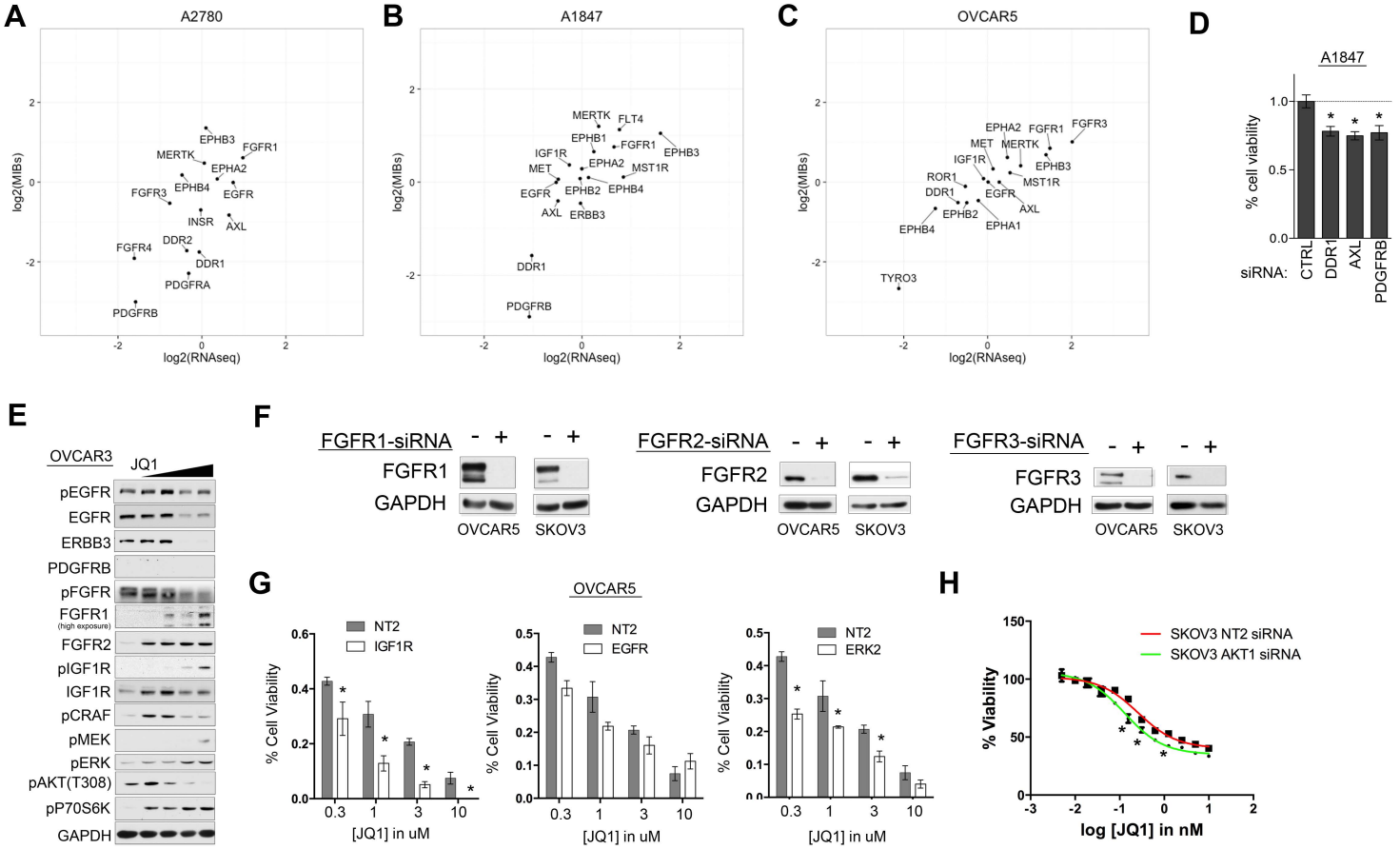
A
A2780
log2(MIBs)
log2(RNAseq)
EPHB3
FGFR1
MERTK
EPHA2
FGFR3
EPHB4
EGFR
INSR
AXL
FGFR4
DDR2
DDR1
PDGFRA
PDGFRB
B
A1847
MERTK
FLT4
EPHB1
FGFR1
EPHB3
IGF1R
MET
EPHA2
MST1R
EGFR
EPHB2
EPHB4
AXL
ERBB3
DDR1
PDGFRB
C
OVCAR5
EPHA2
FGFR1
FGFR3
MET
MERTK
IGF1R
EPHB3
MST1R
ROR1
DDR1
EGFR
AXL
EPHB2
EPHB4
EPHA1
TYRO3
D
A1847
% cell viability
siRNA:
CTRL
DDR1
AXL
PDGFRB

E
OVCAR3
JQ1
pEGFR
EGFR
ERBB3
PDGFRB
pFGFR
FGFR1
(high exposure)
FGFR2
pIGF1R
IGF1R
pCRAF
pMEK
pERK
pAKT(T308)
pP70S6K
GAPDH
F
FGFR1-siRNA
FGFR1
GAPDH
OVCAR5
SKOV3
FGFR2-siRNA
FGFR2
FGFR3-siRNA
FGFR3

G
OVCAR5
NT2
IGF1R
EGFR
ERK2
% Cell Viability
[JQ1] in uM
H
SKOV3 NT2 siRNA
SKOV3 AKT1 siRNA
% Viability
log [JQ1] in nM

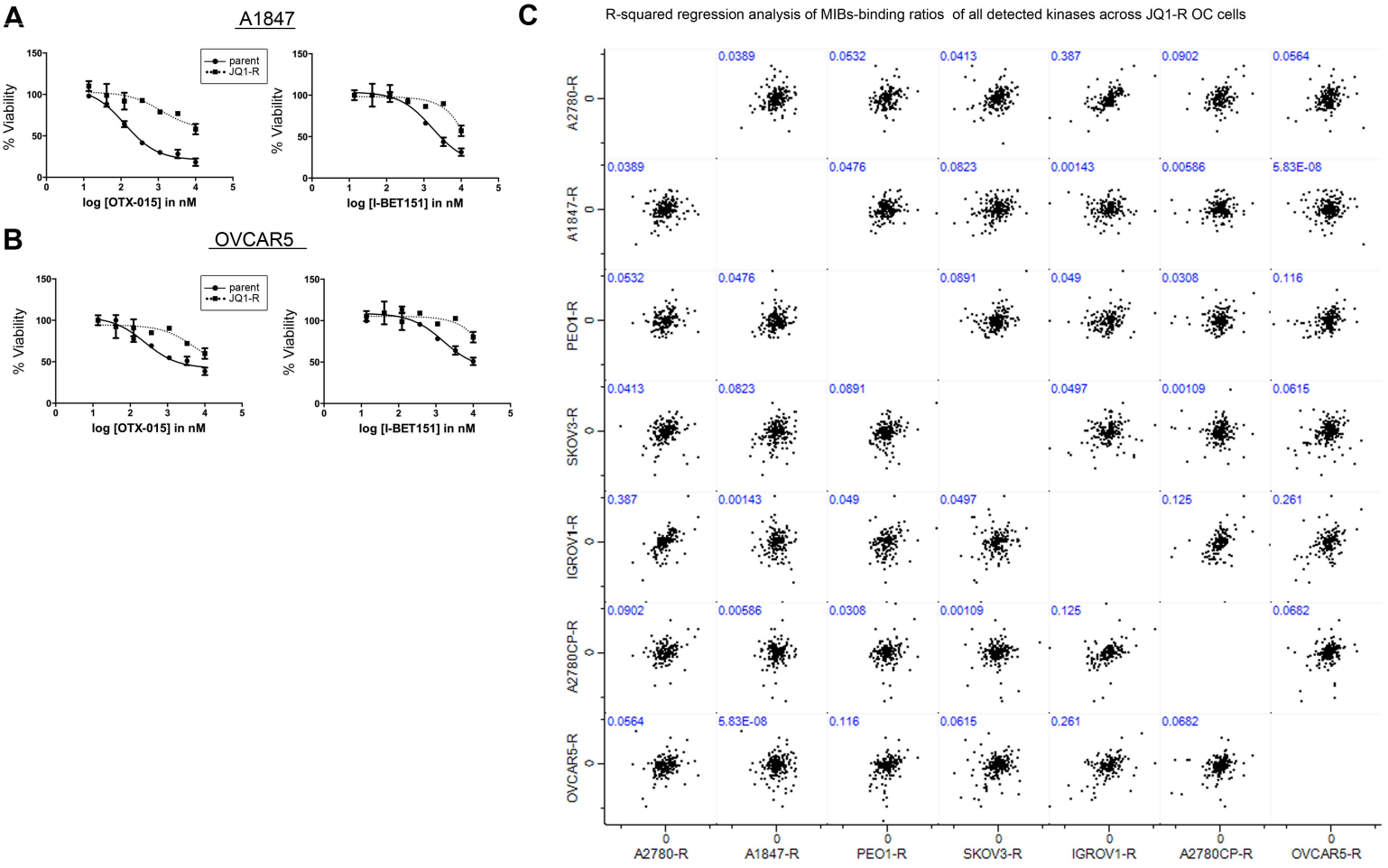
A
A1847
parent
JQ1-R
% Viability
log [OTX-015] in nM
log [I-BET151] in nM
B
OVCAR5
C
R-squared regression analysis of MIBs-binding ratios of all detected kinases across JQ1-R OC cells
A2780-R
A1847-R
PEO1-R
SKOV3-R
IGROV1-R
A2780CP-R
OVCAR5-R

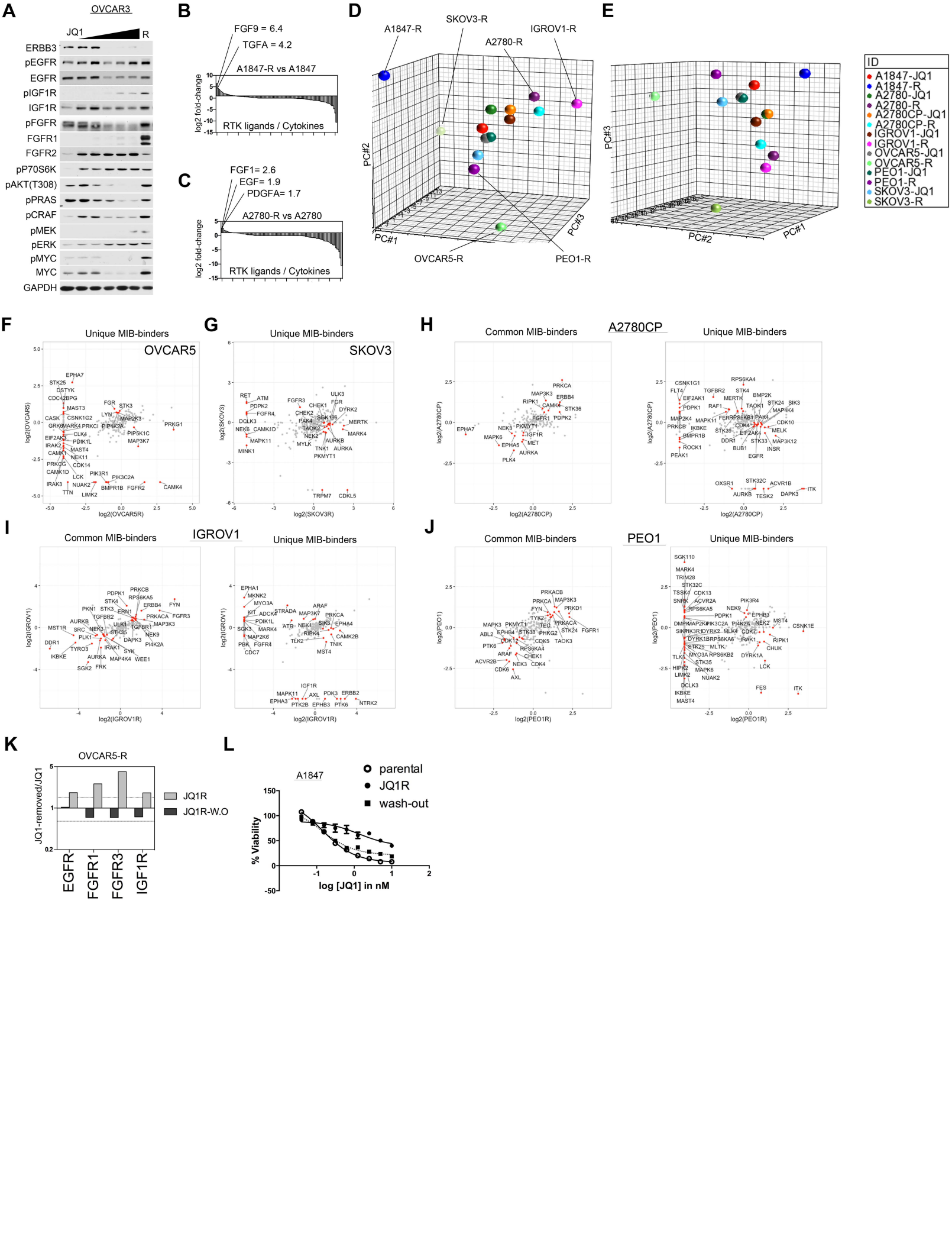
A
OVCAR3
JQ1
R
ERBB3
pEGFR
EGFR
pIGF1R
IGF1R
pFGFR
FGFR1
FGFR2
pP70S6K
pAKT(T308)
pPRAS
pCRAF
pMEK
pERK
pMYC
MYC
GAPDH
B
FGF9 = 6.4
TGFA = 4.2
A1847-R vs A1847
log2 fold-change
RTK ligands / Cytokines
C
FGF1= 2.6
EGF= 1.9
PDGFA= 1.7
A2780-R vs A2780
log2 fold-change
RTK ligands / Cytokines
D
A1847-R
SKOV3-R
IGROV1-R
A2780-R
PC#2
PC#3
PC#1
OVCAR5-R
PEO1-R
E
PC#3
PC#2
PC#1
ID
A1847-JQ1
A1847-R
A2780-JQ1
A2780-R
A2780CP-JQ1
A2780CP-R
IGROV1-JQ1
IGROV1-R
OVCAR5-JQ1
OVCAR5-R
PEO1-JQ1
PEO1-R
SKOV3-JQ1
SKOV3-R
F
Unique MIB-binders
OVCAR5
log2(OVCAR5)
log2(OVCAR5R)
G
Unique MIB-binders
SKOV3
log2(SKOV3)
log2(SKOV3R)
H
Common MIB-binders
A2780CP
Unique MIB-binders
log2(A2780CP)
log2(A2780CP)
I
Common MIB-binders
IGROV1
Unique MIB-binders
log2(IGROV1)
log2(IGROV1R)
log2(IGROV1)
log2(IGROV1R)
J
Common MIB-binders
PEO1
Unique MIB-binders
log2(PEO1)
log2(PEO1R)
log2(PEO1)
log2(PEO1R)
K
OVCAR5-R
JQ1-removed/JQ1
JQ1R
JQ1R-W.O
EGFR
FGFR1
FGFR3
IGF1R
L
A1847
parental
JQ1R
wash-out
% Viability
log [JQ1] in nM

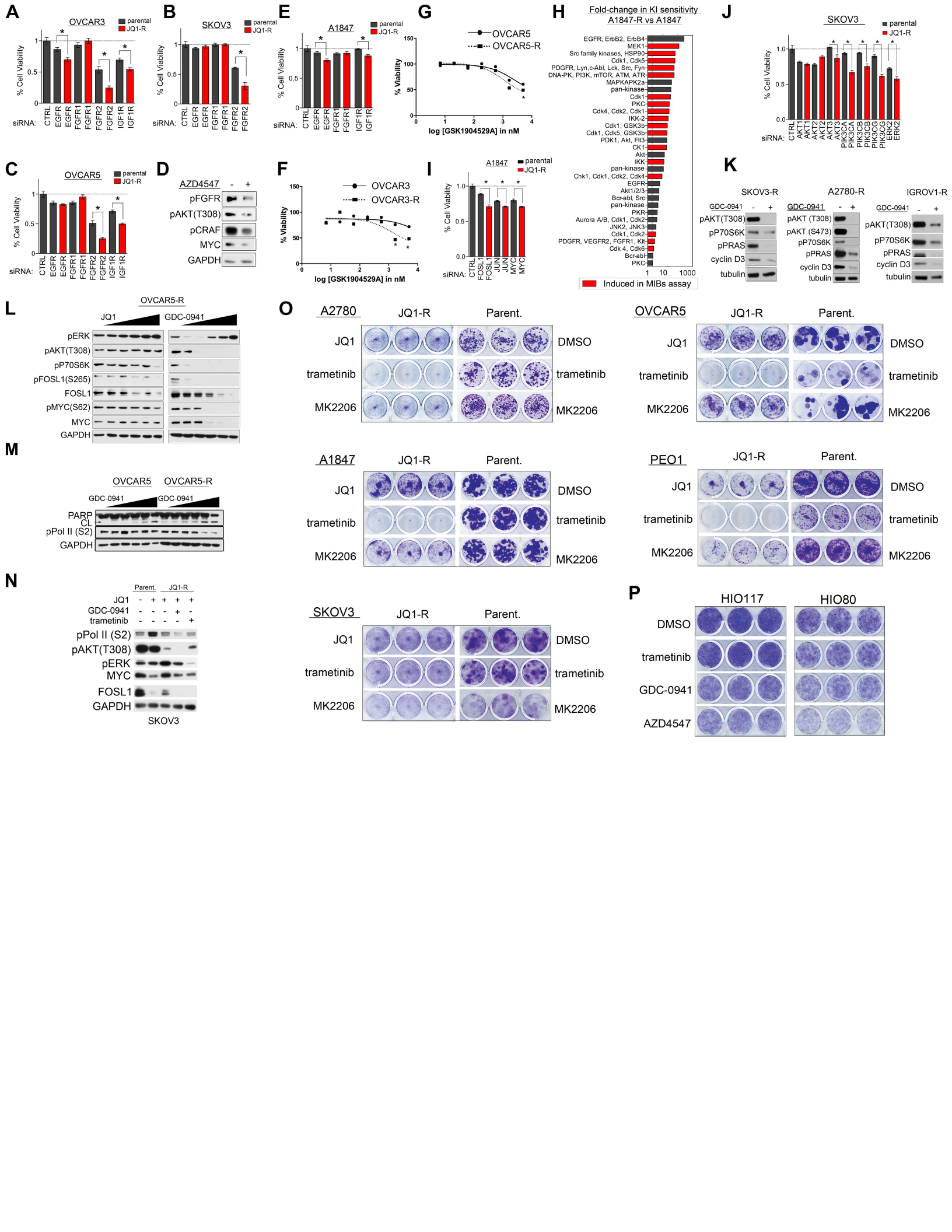
A
OVCAR3
parental
JQ1-R
% Cell Viability
siRNA:
CTRL
EGFR
EGFR
FGFR1
FGFR2
FGFR2
IGF1R
IGF1R
B
SKOV3
C
OVCAR5
D
AZD4547
pFGFR
pAKT(T308)
pCRAF
MYC
GAPDH
E
A1847
F
OVCAR3
OVCAR3-R
% Viability
log [GSK1904529A] in nM
G
OVCAR5
OVCAR5-R
H
Fold-change in KI sensitivity
A1847-R vs A1847
EGFR, ErbB2, ErbB4
MEK1
Src family kinases, HSP90
Cdk1, Cdk5
PDGFR, Lyn,c-Abl, Lck, Src, Fyn
DNA-PK, PI3K, mTOR, ATM, ATR
MAPKAPK2a
pan-kinase
Cdk1
PKC
Cdk4, Cdk2, Cdk1
IKK-2
Cdk1, GSK3b
Cdk1, Cdk5, GSK3b
PDK1, Akt, Flt3
CK1
Akt
IKK
pan-kinase
Chk1, Cdk1, Cdk2, Cdk4
EGFR
Akt1/2/3
Bcr-abl, Src
pan-kinase
PKR
Aurora A/B, Cdk1, Cdk2
JNK2, JNK3
Cdk1, Cdk2
PDGFR, VEGFR2, FGFR1, Kit
Cdk 4, Cdk6
Bcr-abl
PKC
Induced in MIBs assay
I
A1847
J
SKOV3
AKT1
AKT2
AKT2
AKT3
AKT3
PIK3CA
PIK3CA
PIK3CB
PIK3CB
PIK3CG
PIK3CG
ERK2
ERK2
K
SKOV3-R
A2780-R
IGROV1-R
GDC-0941
pAKT(T308)
pP70S6K
pPRAS
cyclin D3
tubulin
pAKT (T308)
pAKT (S473)
L
OVCAR5-R
JQ1
GDC-0941
pERK
pAKT(T308)
pP70S6K
pFOSL1(S265)
FOSL1
pMYC(S62)
MYC
GAPDH
M
OVCAR5
OVCAR5-R
GDC-0941
PARP CL
pPol II (S2)
GAPDH
N
Parent.
JQ1-R
JQ1
GDC-0941
trametinib
pPol II (S2)
pAKT(T308)
pERK
MYC
FOSL1
GAPDH
SKOV3
O
A2780
JQ1-R
Parent.
JQ1
trametinib
MK2206
DMSO
OVCAR5
A1847
PEO1
SKOV3
P
HIO117
HIO80
DMSO
trametinib
GDC-0941
AZD4547

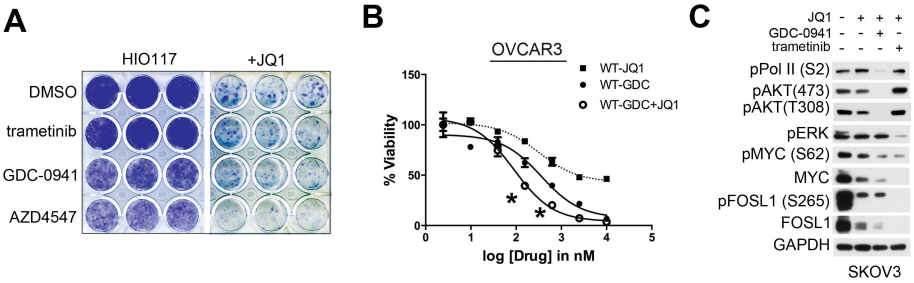
A
HIO117
+JQ1
DMSO
trametinib
GDC-0941
AZD4547
B
OVCAR3
WT-JQ1
WT-GDC
WT-GDC+JQ1
% Viability
log [Drug] in nM
C
JQ1
GDC-0941
trametinib
pPol II (S2)
pAKT(473)
pAKT(T308)
pERK
pMYC (S62)
MYC
pFOSL1 (S265)
FOSL1
GAPDH
SKOV3

SUPPLEMENTARY FIGURE LEGENDS

Figure S1, Related to Figure 1. Dynamic Reprogramming of the Kinome in Response to Targeted BET Protein Inhibition

(A) Proteomic analysis of BET proteins, FOSL1/MYC and RAS/PI3K signaling in OC cell lines determined by blot.
(B-C) OC cells were treated with escalating doses of BETi I-BET151 or PF-1, and cell viability assessed by CellTiter-Glo.
(D) Differential effect of BETi JQ1 (500 nM), I-BET151 (2 μM) or PF-1 (2 μM) on colony formation amongst OC cells determined by crystal violet assays.
(E) Treatment of OVCAR5 cells with escalating doses of JQ1 fails to induce apoptosis to the extent of A2780 cells as determined by Caspase-3-Glo.
(F) Reduced MYC and/or FOSL1 in response to 4 h or 48 h JQ1 (500 nM) treatment as determined by qRT-PCR.
(G-H) Significant overlap in kinome alterations in response to 48 h 500 nM JQ1 or 2 μM I-BET151 in SKOV3 or A1847 cells. Scatterplot depicts SILAC-determined Log_2fold changes in MIB binding as a ratio of JQ1/DMSO or I-BET151/DMSO.

Data presented in (B-C), and (E) are triplicate experiments SEM.

Figure S2, Related to Figure 2. BET Protein Inhibition Induces Variable Kinome Responses Across Ovarian Cancer Cells

(A-C) Scatterplot of kinases uniquely detected to be increased (≥1.5-fold) or repressed (≤1.5-fold) by MIB-based proteomics (in red) and not by RNAseq analysis. A2780, A1847, and OVCAR5 cells were treated with JQ1 (500 nM) for 48 h.
(D) Go ontology of MIBs-defined kinome changes following 48 h JQ1 (500 nM) in OC cells.
(E) Principal component analysis of MIBs-defined kinome response profiles across OC cell lines treated with JQ1 (500nM) for 48 h comparing PC2 vs PC3.
(F) R-squared regression analysis of MIBs-binding ratios post JQ1 of all detected kinases across the 8 OC cell lines. Analysis and plots performed in Perseus. Top two R-squared values depicted in red box.
(G-H) Scatterplot of common JQ1 induced (≥1.5-fold) or repressed (≤1.5-fold) MIB-binding ratios (in red) comparing JQ1-sensitive A2780 vs. A1847 and JQ1-resistant OVCAR5 vs. SKOV3 kinome responses.

Figure S3, Related to Figure 3. Rewiring of the Receptor Tyrosine Kinome Following BET Bromodomain Inhibition

(A-C) Comparison of RTK response of OC cells to JQ1 (500 nM) 48 h as determined by MIB/MS and RNAseq. Scatterplot depicts Log_2 fold changes in MIB binding or RNAseq as a ratio of JQ1/DMSO.
(D) Knockdown of RTKs DDR1, AXL, or PDGFRB decrease cell viability in A1847 cells.
(E) Treatment of OVCAR3 cells with escalating doses of JQ1 reduces EGFR, ERBB3, and pFGFR levels as determined by blot.
(F) RNAi-mediated knockdown of FGFRs in OVCAR5 and SKOV3 confirmed by blot.
(G) Knockdown of IGF1R or ERK2, but not EGFR, sensitizes OVCAR5 to BET protein inhibition. Cell viability was assessed in response to escalating doses of JQ1 for 72 h in the presence or absence of siRNA-knockdown.
(H) RNAi-mediated knockdown of AKT1 sensitizes SKOV3 cells to JQ1. Cell viability was assessed in response to escalating doses of JQ1 for 72 h in the presence or absence of siRNA-knockdown.

Data presented in (D), (G), and (H) are triplicate experiments SEM. *$p \leq 0.05$ by student's t-test.

Figure S4, Related to Figure 4. Ovarian Cancer Cells Acquire Resistance to Chronic BET Protein Inhibition

(A-B) A1847 and OVCAR5 JQ1-R cells exhibit cross-resistance to other BET protein inhibitors. JQ1-R cells were treated with escalating doses of I-BET151 or OTX-015, and cell viability assessed by CellTiter-Glo. Triplicate experiments SEM.
(C) R-squared regression analysis of MIBs-binding ratios of all detected kinases across the 7 OC cells following chronic JQ1 exposure. Analysis and plots performed in Perseus.

Figure S5, Related to Figures 5. Chronic Exposure to JQ1 Activates an Assortment of Kinase Signaling Cascades That Are Reversible

(A) OVCAR3 cells chronically exposed to JQ1 activate FGFR, IGF1R and EGFR RTKs and their downstream AKT-ERK signaling as shown by blot. Parental cells treated with escalating doses of JQ1 for 48 h or resistant cells (isolated from western blot in Figure S3E). Lane (R), OVCAR3-R cells continually grown in 500 nM JQ1.

(B-C) Induction of RTK ligands in A1847 and A2780 following chronic exposure to JQ1. Line graph depicts Log_2 fold changes in RNA levels as a ratio of JQ1-R/parental cells determined by RNAseq.

(D-E) Principal component analysis of MIBs-defined kinome profiles of OC cell lines treated with JQ1 for 48 h or chronically treated with JQ1 (500 nM) depicts the heterogeneity between the short-term and chronic kinome responses. Different views of the 3D PCA plots are shown to illustrate the grouping of kinome profiles.

(F-J) Comparison of MIB-binding ratios of kinases induced (≥1.5-fold) or repressed (≤1.5-fold) following 48 h or chronic JQ1 therapy. Scatterplots depict common or unique SILAC-determined Log_2 fold changes in MIB binding (in red) as a ratio of JQ1 48-h/DMSO or JQ1-R/ parental.

(K) JQ1-induced FGFR1, FGFR3 and IGF1R activity is reversible in OVCAR5-R cells. MIB/MS-defined kinome profiles of OC cell lines following chronic JQ1 (500 nM) treatment or 48 h post JQ1 removal (wash-out, WO). Line graph depicts SILAC-determined Log_2 fold changes in MIB binding as a ratio of JQ1-R/ parental or JQ1-R-WO / JQ1-R.

(L) A1847 parental, JQ1-R, or JQ1 wash-out cells were treated with escalating doses of JQ1. Cell viability was assessed by CellTiter-Glo. Triplicate experiments SEM.

Figure S6, Related to Figure 6. Ovarian Cancer Cells Chronically Exposed to JQ1 Acquire Dependency on RTK, PI3K and/or ERK Signaling and Exhibit Exquisite Sensitivity to Kinase Inhibitors Targeting These Pathways

(A-C) JQ1-R cells are more dependent on RTK signaling than parental cells. Parental and JQ1-R cells were transfected with siRNAs targeting RTKs and cultured for 72 h. JQ1-R treated cell viabilities normalized to untreated JQ1-R. Cell viability was assessed by CellTiter-Glo.

(D) FGFR inhibition blocks downstream RAF-AKT signaling in SKOV3-R cells. Cells were treated with AZD4547 (1 μM) for 48 h and signaling assessed by blot.

(E) A1847-R cells are more dependent on EGFR and IGF1R signaling than parental cells. Parental and JQ1-R cells were transfected with siRNAs targeting RTKs and cultured for 72 h. JQ1-R treated cell viabilities normalized to untreated JQ1-R. Cell viability was assessed by CellTiter-Glo.

(F-G) OVCAR3 and OVCAR5 JQ1-R cells show enhanced sensitivity to IGF1R inhibitor (GSK1904529A) relative to parental cells. JQ1-R treated cell viabilities normalized to DMSO treated JQ1-R cells. Cell viability was assessed by CellTiter-Glo.

(H) A1847-R cells show enhanced sensitivity to targeted MEK and PI3K/mTOR/AKT inhibitors relative to parental cells in an unbiased kinase inhibitor screen. Fold-change in sensitivity to kinase inhibitors determined A1847-R relative to parental cells. Kinase inhibitors in red target kinases identified by MIBs to be elevated in the JQ1-R cells relative to parental cells.

(I) Acquired dependency on MYC, FOSL1 and JUN transcription factors in A1847-R cells. Parental A1847 cells or A1847-R cells were transfected with siRNAs targeting MYC, FOSL1 or JUN and cultured for 72 h. JQ1-R knockdown cells were normalized to JQ1-R cells transfected with non-targeting siRNA.

(J) Acquired dependency on PI3K in SKOV3-R cells. Parental cells or JQ1-R cells were transfected with siRNAs targeting PI3Ks, AKTs, and ERK2 and cultured for 72 h. JQ1-R treated cell viabilities normalized to JQ1-R cells transfected with non-targeting siRNA.

(K) Treatment of SKOV3, A2780, or IGROV1 JQ1-R cells with GDC-0941 (500 nM) blocks PI3K/mTOR signaling as determined by blot.

(L-M) Treatment of OVCAR5-R cells with GDC-0941 blocks ERK and AKT signaling and represses MYC/FOSL1 protein levels to a greater extent than JQ1 treatment, resulting in apoptosis and loss of RNA pol II (S2) phosphorylation. JQ1 resistant cells were treated with escalating doses of JQ1 or GDC-0941 for 48 h and protein levels determined by western blot.

(N) Treatment of SKOV3-R cells with GDC-0941 (500 nM) or trametinib (10 nM) for 48 h inhibits AKT or ERK signaling, decreases FOSL1 and/or MYC and blocks RNA pol II (S2) phosphorylation.

(O) Blockade of MEK-ERK signaling inhibits colony formation in the majority of JQ1-R OC cells to a greater extent than in parental cells. Long-term 14-day colony formation assay of JQ1-R OC cells treated with DMSO (500 nM, JQ1), trametinib (10 nM) or MK2206 (500 nM) as determined by crystal violet assays. Drug doses were selected based on inhibition of targeted kinase and downstream targets.

(P) Treatment of non-tumorigenic immortalized human ovarian surface epithelial cells with AZD4547 (1 μM), GDC-0941 (500 nM) or trametinib (10 nM) for 14 days and colony formation assessed by crystal violet.

Data presented in (A-C), (E), (F-G), (I) and (J) are triplicate experiments SEM. *p ≤0.05 by student's t-test.

Figure S7, Related to Figure 7. Combination Therapies Targeting RTK, PI3K or ERK Signaling Concurrently With BET Protein Inhibitors Enhance Growth Inhibition in OC Cells

(A) Co-treatment of non-tumorigenic immortalized human ovarian surface epithelial cells with JQ1 (200 nM) and either AZD4547 (1 μM), GDC-0941 (500 nM), or trametinib (10 nM) for 14 days, and colony formation assessed by crystal violet.

(B) OVCAR3 cells treated with combination of GDC-0941 and JQ1 block cell growth to a greater extent than single agent treatments. Cells were treated with escalating doses of JQ1, GDC-0941 or the combination of GDC-0941 for 72 h, and cell viability assessed by CellTiter-Glo. Triplicate experiments SEM. *$p \leq 0.05$ by student's t-test.

(C) Co-treatment of SKOV3 cells with JQ1 and either GDC-0941 (500 nM) or trametinib (10 nM) reduces MYC and/or FOSL1 levels to a greater extent than single agents as depicted by blot.

Table S1, related to Figures 1, 2, 4, 5, S2, S3, and S5: Raw RNAseq reads (excel spreadsheet): Values are normalized FPKM reads (see Supplemental Experimental Procedures). Tabs:

A2780 RNAseq JQ1 48h: A2780 cells treated +/- JQ1 (500 nM) for 48 h.

OVCAR5 RNAseq JQ1 48h: OVCAR5 cells treated +/- JQ1 (500 nM) for 48 h.

A1847 RNAseq JQ1 48h: A1847 cells treated +/- JQ1 (500 nM) for 48 h.

A2780 JQ1 48h RNAseq Kinome: RNAseq reads of protein kinome in A2780 cells treated +/- JQ1 (500 nM) for 48 h.

OVCAR5 JQ1 48h RNAseq Kinome: RNAseq reads of protein kinome in OVCAR5 cells treated +/- JQ1 (500 nM) for 48 h.

A1847 JQ1 48h RNAseq Kinome: RNAseq reads of protein kinome in A1847 cells treated +/- JQ1 (500 nM) for 48 h.

A2780 JQ1 48h MIBs vs RNAseq: Comparison of MIBs-determined SILAC ratios and RNAseq-defined expression changes in kinome in A2780 cells treated +/- JQ1 (500 nM) for 48 h.

OVCAR5 JQ1 48h MIBs vs RNAseq: Comparison of MIBs-determined SILAC ratios and RNAseq-defined expression changes in kinome in OVCAR5 cells treated +/- JQ1 (500 nM) for 48 h.

A1847 JQ1 48h MIBs vs RNAseq: Comparison of MIBs-determined SILAC ratios and RNAseq-defined expression changes in kinome in A1847 cells treated +/- JQ1 (500 nM) for 48 h.

A1847 JQ1R RNAseq Kinome: RNAseq reads of protein kinome in A1847 JQ1R cells relative to A1847 parental cells.

A2780 JQ1R RNAseq Kinome: RNAseq reads of protein kinome in A2780 JQ1R cells relative to A2780 parental cells.

A1847 JQ1R MIBs vs RNAseq: Comparison of MIBs-determined SILAC ratios and RNAseq-defined expression changes in kinome in A1847 JQ1R and A1847 parental cells.

A2780 JQ1R MIBs vs RNAseq: Comparison of MIBs-determined SILAC ratios and RNAseq-defined expression changes in kinome in A2780 JQ1R and A2780 parental cells.

A1847 JQ1R RNAseq RTK ligands: Expression changes of RTK ligands and cytokines in A1847 JQ1R cells relative to parental A1847 cells.

A2780 JQ1R RNAseq RTK ligands: Expression changes of RTK ligands and cytokines in A2780 JQ1R cells relative to parental A2780 cells.

Table S2, related to Figures 1, 2, 3, 4, 5, S1, S2, S3, S4 and S5: Raw MIB/MS Ratios (excel spreadsheet). Tabs:

SILAC Log2 MIB ratios JQ1 48h: MIB/MS runs of IGROV1, PEO1, OVCAR3, A2780, A1847, SKOV3, OVCAR5 and A2780CP OC cells treated with JQ1 (500 nM) for 48 h from Figure 1I.

Average Log2 SILAC MIB ratios: Averaged SILAC MIB/MS ratios for each of the 8 OC cells.

SKOV3 JQ1 vs IBET151 48h MIBs: Comparison of MIB/MS ratios in SKOV3 cells treated with JQ1 (500 nM) or I-BET-151 (2 μM) for 48 h.

A1847 JQ1 vs IBET151 48h MIBs: Comparison of MIB/MS ratios in A1847 cells treated with JQ1 (500 nM) or I-BET-151 (2 μM) for 48 h.

One-paired T-test all OC cells: Statistical analysis of common MIB-binding changes across the 8 OC cells in response to JQ1 (500 nM) 48 h treatment from Figure 2D.

SILAC Ratios JQ1R vs Parental: MIB/MS runs and SILAC-determined MIB-binding ratios of A1847, OVCAR5, SKOV3 and A2780 JQ1-resistant cells relative to parental cells.

SuperSILAC Ratios JQ1RvsParenta: MIB/MS runs and SILAC-determined MIB-binding ratios of PEO1, IGROV1 and A2780CP JQ1-resistant cells relative to parental cells (See Supplemental Experimental Procedures).

Average SILAClog2Ratios JQ1RvsP: Averaged SILAC-determined MIB/MS ratios of JQ1R cells relative to parental cells from Figure 4G.

Table S3, related to Figure 7. Raw Drug Synergy Values (excel spreadsheet). Combination Index (CI) values were established by the Chou-Talalay method (See Supplemental Experimental Procedures). Tabs:

CI value TABLE 1: Table showing the individual CI's for JQ1, GDC-0941 and the combination of JQ1 and GDC-0914 of PDX-derived EOC cells OC-1, OC-20, OC-29, OC-38 and OC-16.

OC-29-OC38-OC16: CellTiter-Blue values for OC-29, OC-38 and OC-16 treated with escalating doses of JQ1, GDC-0941 and the combination of JQ1 and GDC-0914.

OC29-38-16 CI values: Calculations related to generated CI values for OC-29, OC-38 and OC-16.

OC-1: CellTiter-Blue values for OC-1 and calculations related to generated CI values.

OC-20: CellTiter-Blue values for OC-20 and calculations related to generated CI values.

SUPPLEMENTAL EXPERIMENTAL PROCEDURES

Cell Lines

Cell lines were verified by IDEXX laboratories and maintained in RPMI-1640 + 10% FBS, 5µg/ml Insulin, 100 U/ml Penicillin-Streptomycin and 2mM GlutaMAX at 37^{o}C in a 5% CO_2 incubator. HIO-80 and HIO-117 ovarian surface epithelial cells were a generous gift supplied by Dr. Andrew Godwin (The University of Kansas) and were maintained in MCDB 105/Media 199 + 5% FBS, 7.5 µg/ml Insulin, 100 U/ml Penicillin-Streptomycin and 2mM GlutaMAX. To generate JQ1-resistant cell lines, parental cells were chronically exposed to 500 nM JQ1 and resistant clones were isolated and propagated in the continued presence of 500 nM JQ1. For SILAC labeling, cells were grown for seven doublings in arginine- and lysine-depleted media supplemented with either unlabeled L-arginine (84 mg/L) and L-lysine (48 mg/L) or equimolar amounts of heavy isotope labeled [$^{13}C_6$,$^{15}N_4$]arginine (Arg^{10}) and [$^{13}C_6$]lysine (Lys^{6}) (Sigma) as described previously (Ong SE, 2002).

Compounds

BET protein inhibitors JQ1, I-BET151 or OTX-015 were purchased from Selleckchem. Trametinib (GSK1120212), GDC-0941, MK2206, Vx-11e, GSK1904529A, AZD4547, and BGJ398 were purchased from Selleckchem. Purvalanol B was purchased from Abcam. PP58 (Klutchko, 1998) and VI16832 (Daub et al., 2008) were custom synthesized according to previously described methods by The Center for Combinatorial Chemistry and Drug Discovery, Jilin University, P.R. China. CTx-0294885 (Zhang et al., 2013) was synthesized according to previously described methods by Moulder Drug Discovery Group, Temple University. Conjugation of inhibitors to beads was performed by carbodiimide coupling to ECH Sepharose 4B (CTx-0294885, VI16832 and PP58) or EAH Sepharose 4B (purvalanol B) (GE Healthcare).

Western Blotting

Cell lysates were subjected to SDS-PAGE chromatography and transferred to nitrocellulose membranes before western blotting with primary antibodies. Antibodies against AKT1, AKT2, pAKT (T308), pAKT (S473), Aurora A, DDR1, DDR2, EGFR, pEGFR (Y1068), pEGFR (Y845), pEGFR(Y1173), pERK1/2 (T202/Y204), ERBB2, pERBB2 (Y1221/1222), ERBB3, FGFR1, FGFR4, pFGFR (Y653/654), FOSL1, pFOSL1 (S265), GAPDH, ERBB4, JAK1, pSAPK/JNK (T183/Y185), KIT, pKIT(Y719), pLATS1(S909), pMEK1/2 (S217/S221), MEKK3, MERTK, MST1, pMST1 (T183), MST2, MYC, pMYC(S62), IGF1R, INSRB, pIGF1R (Y1131)/pINSRB (Y1146), PDGFRB, PDGFRA, pPDGFRA/B (Y849, Y857), pP70S6 kinase (T389), pPRAS40 (T246), PARP1, pRNA pol II (S2), pRSK1 (T359/S363), pRAF (S338), RIPK1, pRIPK1(S166), pSRC (Y416), pSMAD2/3(S465/467), pSTAT3(Y705), YAP1, pYAP1(S127) were obtained from Cell Signaling Technology. Antibodies for BRD2, BRD3, ERK1, ERK2, FGFR2, FGFR3 and TGFBR1 were obtained from Santa Cruz Biotechnology. ACVR2A antibody was obtained from Abcam. The antibody against BRD4 was from Active Motif. Secondary HRP-anti-rabbit and HRP-anti-mouse were obtained from ThermoFisher Scientific. SuperSignal West Pico and Femto Chemiluminescent Substrates (Thermo) were used to visualize blots.

RTK Arrays

Cells were harvested in RTK array lysis buffer containing 20 mM Tris-HCl (pH 8.0), 1% NP-40, 10% glycerol, 137 mM NaCl, 2 mM EDTA, 1X EDTA-free protease inhibitor cocktail (Roche), and 1% each of phosphatase inhibitor cocktails 1 and 2 (Sigma). After incubating on ice for 20 minutes, cell debris was pelleted at 4° C. Lysates (500 µg protein) were applied to R&D Systems Proteome Profiler™ Human Phospho-RTK antibody arrays. Washing and secondary antibody steps were performed according to the manufacturer's instructions. RTK arrays were visualized by SuperSignal West Pico and Femto Chemiluminescent Substrate (Thermo Scientific).

Growth and Apoptosis Assays

For short-term growth assays, 1000-2000 cells were plated per well in 96-well plates and allowed to adhere and equilibrate overnight. Drug was added the following morning and after 72 h of drug treatment, cell viability was assessed using the CellTiter-Glo Luminescent cell viability assay according to manufacturer (Promega). Students t tests were performed for statistical analyses and p

values ≤ 0.05 were considered significant. For colony formation assays, cells were plated in 6 or 24-well dishes (200-1000 cells per well) and incubated overnight before continuous drug treatment for 14 days, with drug and media replaced twice weekly. At the end of treatment, cells were rinsed with PBS and fixed with chilled methanol for 10 min at -20°C. Methanol was removed by aspiration, and cells were stained with 0.5% crystal violet in 20% methanol for 20 min at room temperature, washed with distilled water, and scanned. Apoptosis was determined 48 hrs following drug treatment using Caspase 3/7 Glo assay according to manufacturer's instructions.

MIBs Preparation and Chromatography

Experiments using MIB/MS were performed as previously described (Duncan et al., 2012; Stuhlmiller et al., 2015). Briefly, cells or tumors were lysed on ice in buffer containing 50 mM HEPES (pH 7.5), 0.5% Triton X-100, 150 mM NaCl, 1 mM EDTA, 1 mM EGTA, 10 mM sodium fluoride, 2.5 mM sodium orthovanadate, 1X protease inhibitor cocktail (Roche), and 1% each of phosphatase inhibitor cocktails 2 and 3 (Sigma). Particulate was removed by centrifugation of lysates at 13,000 rpm for 10 minutes at 4°C and filtration through 0.2 μm syringe filters. Protein concentrations were determined by BCA analysis (Thermo). Equal volumes of SILAC-labeled heavy (5mg) and light (5mg) lysates were mixed and endogenous kinases were isolated by flowing lysates over kinase inhibitor-conjugated Sepharose beads (purvalanol B, VI16832, PP58 and CTx-0294885 beads were used) in 10 ml gravity-flow columns. Due to difficulties in adapting PEO1, IGROV1 and A2780CP JQ1-R cells into SILAC media conditions, a super-SILAC metabolic labeling technique was employed to assess relative quantitation differences between parental PEO1, IGROV1 or A2780CP and JQ1-R samples (Neubert and Tempst, 2010). Our super-SILAC cocktail consisted of the equal mixture of OC cell lines (A2780, PEO1, A1847, IGROV1 and OVCAR5). Differences in MIB-binding between parental and JQ1-resistant cells was determined by taking the ratio of JQ1-R:super-SILAC mix relative to the ratio of parental: super-SILAC mix. After 2x10 ml column washes in high-salt buffer and 1x10 ml wash in low-salt buffer (containing 50 mM HEPES (pH 7.5), 0.5% Triton X-100, 1 mM EDTA, 1 mM EGTA, and 10 mM sodium fluoride, and 1M NaCl or 150 mM NaCl, respectively), retained kinases were eluted from the column by boiling in 2x500 μl of 0.5% SDS, 0.1 M TrisHCl (pH 6.8), and 1% 2-mercaptoethanol. Eluted peptides were reduced by incubation with 5 mM DTT at 60°C for 25 minutes, alkylated with 20 mM iodoacetamide at room temperature for 30 minutes in the dark and alkylation was quenched with DTT. Samples were concentrated to approximately 100 μl with Millipore 10kD cutoff spin concentrators. Detergent was removed by chloroform/methanol extraction, and the protein pellet was resuspended in 100 mM ammonium bicarbonate and digested with sequencing-grade modified trypsin (Promega) overnight at 37°C. SILAC-labeled kinase peptides were cleaned with PepClean C18 spin columns (Thermo), and subsequent LC/MS analysis was performed.

Mass Spectrometry and Spectra Analysis

Proteolytic peptides were resuspended in 0.1% formic acid and separated with a Thermo RSLC Ultimate 3000 on a Thermo Easy-Spray C18 PepMap 75μm x 50cm C-18 2 μm column with a 235 min gradient of 4-25% acetonitrile with 0.1% formic acid at 300 nL/min and 50°C. Eluted peptides were analyzed by a Thermo Q Exactive plus mass spectrometer utilizing a top 15 methodology in which the 15 most intense peptide precursor ions were subjected to fragmentation. The AGC for MS1 was set to $3x10^6$ with a max injection time of 120 ms, and the AGC for MS2 ions was set to $1x10^5$ with a max injection time of 150 ms and the dynamic exclusion was set to 90 s. Raw files were searched against the Uniprot/Swiss-Prot database with SEQUEST HT on Proteome Discoverer software (v1.4). Proteins were accepted when ≥1 unique peptide was identified at 1% FDR and only peptides with high confidence were considered for quantitation.

Statistical Analysis of MIB/MS

For JQ1-induced MIBs signatures, we performed at least 2 biological MIB/MS experiments using both SILAC H/L and L/H. Q-Exactive data was analyzed as follows: for a total of *p* unique kinases, we computed the pooled protein ratio and p-value across the replicates. For each replicate, we identified kinases that exhibit statistically significant changes in expression based on stepup-adjusted p-values at FDR of 0.05 to account for multiple comparisons. Principle component analysis (PCA) of kinome profiling MIBs-values was performed using Partek Genomics Suite (Partek Inc.). Visualization of MIBs-kinome signatures using PCA plots, Box-and-whiskers plots or Log_2 ratio heat maps were generated using Partek Genomics Suite. R-squared regression analysis MIB/MS runs were performed on Perseus Software v 1.5.2.6. Scatterplots comparing MIB-binding ratios were generated using R statistical software. Only kinases that were captured in independent experiments were considered for statistical analysis, and resulting statistically significant kinases were combined to generate signatures.

qRT-PCR

GeneJET RNA purification kit (Thermo Scientific) was used to isolate RNA from cells according to manufacturer's instructions. qRT-PCR on diluted cDNA was performed with inventoried TaqMan® Gene Expression Assays on the Applied Biosystems 7500 Fast Real-Time PCR System. MYC (Assay ID: Hs04187685_m1) and FOSL1 (Assay ID: Hs00153408_m1) TaqMan Gene Expression Assay probes (Life Technologies) were used to assess changes in gene expression.

RNAi Knockdown Studies

siRNA transfections were performed using 50 nM siRNA duplex, and the reverse transfection protocol (2000-5000 cells per well were added to 96 well plates with media containing the drug, siRNA, and transfection reagent) with Dharmafect 1 reagent (GE Healthcare) according to the manufacturer's instructions. Cells were allowed to grow for 72 h post-transfection prior to CellTiter Glo (Promega) analysis. Viability at each concentration was determined by dividing the value at that concentration by the value of the DMSO control of the respective cell line (WT values are compared to the WT DMSO control; JQ1R cells are compared to the JQ1R control, etc.). Two-to-three independent experiments were performed with each cell line and siRNA. Students t tests were performed for statistical analyses and p values ≤ 0.05 were considered significant. All siRNAs were siGENOME/SMARTpool (GE Dharmacon); AKT1 (M-003000-03), AKT2 (M-003001-02), AKT3 (M-003002-02), PIK3CA (M-003018-03), PIK3CB (M-003019-02), PIK3CG (M-005274-02), ERK2 (MAPK1) (M-003555-04), BRD4 (M-004937-02), BRD3 (M-004936-01), BRD2 (M-004935-02), EGFR (M-003114-03), FGFR1 (M-003131-03), FGFR2 (M-003132-04), FGFR3 (M-003133-01), IGF1R (M-003012-05), FOSL1 (M-004341-04), JUN (M-003268-03), MYC (M-003282-07), Non-Targeting siRNA Pool #2 (D-001206-14-05).

Kinase Inhibitor Screen

Inhibitor screen on parental or JQ1-resistant A1847 cells was carried out according to previous methods (Fink et al., 2015). Briefly, twenty-four hours after cell seeding in 384-well plates, cells were treated with DMSO or one of eight doses of kinase inhibitors (final concentration range 64 pm- 5 μM). The kinase inhibitors were added by manual pin transfer, and the final concentration of DMSO was <0.3% for all inhibitor concentrations. The kinase inhibitor library was purchased from EMD Millipore.

RNA Sequencing

The sequencing libraries were constructed from 500 ng of total RNA using the Illumina TruSeq RNA Sampleprep kit V2 (Illumina) following the manufacturer instruction. The fragment size of RNAseq libraries was verified using the Agilent 2100 Bioanalyzer (Agilent), and the concentrations were determined using a Qubit instrument (LifeTech). The libraries were loaded onto the Illumina HiSeq 2500 at 8 pM and run the rapid mode for 2x40 bp paired end sequencing. The fastq files were generated on the Illumina BaseSpace, and further data analysis was performed using the TopHat for read alignment and the Cufflinks Assembly & DE for gene expression assessment (Trapnell et al., 2012).

Drug Synergy Testing

GDC-0941 and JQ1 were tested individually or in combination. Ovarian cancer PDX-derived cells grown on J2 feeder cells (Liu et al., 2012) were plated at 3000 cells per well in 96-well plates. After 24 hours of incubation, cells were treated with serial dilutions of individual drugs or combinations of two drugs at a constant molar ratio. After 72 hours of incubation, cell viability was measured with CellTiter-Blue (Promega) using an EnVision Plate Reader (Perkin Elmer). Combination Index (CI) values were established by the Chou-Talalay method (Chou, 2010) (calculated using the CompuSyn software package (ComboSyn).

SUPPLEMENTAL REFERENCES

Chou, T.-C. (2010). Drug combination studies and their synergy quantification using the Chou-Talalay method. Cancer Res. *70*, 440-446.

Daub, H., Olsen, J.V., Bairlein, M., Gnad, F., Oppermann, F.S., Körner, R., Greff, Z., Kéri, G., Stemmann, O., and Mann, M. (2008). Kinase-selective enrichment enables quantitative phosphoproteomics of the kinome across the cell cycle. Mol. Cell *31*, 438-448.

Fink, L.S., Beatty, A., Devarajan, K., Peri, S., and Peterson, J.R. (2015). Pharmacological profiling of kinase dependency in cell lines across triple-negative breast cancer subtypes. Mol. Cancer Ther. *14*, 298-306.

Klutchko, S.R., Hamby, J. M., Boschelli, D. H., Wu, Z., Kraker, A. J., Amar, A. M., Hartl, B., G., Shen, C., Klohs, W. D., and Steinkampf, *et al.* (1998). 2-substituted aminopyrido[2,3-d]pyrimidin-7(8h)-ones. Structure-activity relationships against selected tyrosine kinases and in vitro and in vivo anticancer activity. J. Med. Chem. *41*, 3276-3292.

Liu, X., Ory, V., Chapman, S., Yuan, H., Albanese, C., Kallakury, B., Timofeeva, O.A., Nealon, C., Dakic, A., Simic, V., *et al.* (2012). ROCK inhibitor and feeder cells induce the conditional reprogramming of epithelial cells. Am. J. Pathol. *180*, 599-607.

Neubert, T.A., and Tempst, P. (2010). Super-SILAC for tumors and tissues. Nat. Meth. *7*, 361-362.

Ong SE, B.B., Kratchmarova I, Kristensen DB, Steen H, Pandey A, Mann M. (2002). Stable isotope labeling by amino acids in cell culture, SILAC, as a simple and accurate approach to expression proteomics. Mol. Cell Proteomics *1*, 376-386.

Trapnell, C., Roberts, A., Goff, L., Pertea, G., Kim, D., Kelley, D.R., Pimentel, H., Salzberg, S.L., Rinn, J.L., and Pachter, L. (2012). Differential gene and transcript expression analysis of RNA-seq experiments with TopHat and Cufflinks. Nat. Protoc. *7*, 562-578.

Zhang, L., Holmes, I.P., Hochgräfe, F., Walker, S.R., Ali, N.A., Humphrey, E.S., Wu, J., de Silva, M., Kersten, W.J.A., Connor, T.*, et al.* (2013). Characterization of the novel broad-spectrum kinase inhibitor CTx-0294885 as an affinity reagent for mass spectrometry-based kinome profiling. J. Proteome Res. *12*, 3104-3116.